nature chemistry

ARTICLES

https://doi.org/10.1038/s41557-020-00576-z

Check for updates

Enantioselective C(sp^3)–C(sp^3) cross-coupling of non-activated alkyl electrophiles via nickel hydride catalysis

Srikrishna Bera[1,2], Runze Mao[1,2] and Xile Hu[1]✉

Cross-coupling of two alkyl fragments is an efficient method to produce organic molecules rich in sp^3-hybridized carbon centres, which are attractive candidate compounds in drug discovery. Enantioselective C(sp^3)–C(sp^3) coupling is challenging, especially of alkyl electrophiles without an activating group (aryl, vinyl, carbonyl). Here, we report a strategy based on nickel hydride addition to internal olefins followed by nickel-catalysed alkyl–alkyl coupling. This strategy enables the enantioselective cross-coupling of non-activated alkyl halides with alkenyl boronates to produce chiral alkyl boronates. Employing readily available and stable olefins as pro-chiral nucleophiles, the coupling proceeds under mild conditions and exhibits broad scope and high functional-group tolerance. Applications for the functionalization of natural products and drug molecules, as well as the synthesis of chiral building blocks and a key intermediate to (*S*)-(+)-pregabalin, are demonstrated.

In drug discovery, it has been recognized that organic compounds with a greater 3D shape than flat aromatics have a higher chance of succeeding as drug candidates[1,2]. The fraction of sp^3 carbons in a molecule has been suggested as a descriptor for its 3D shape[1]. Because high-throughput synthesis has become a standard practice in the pharmaceutical industry, methods introducing sp^3 carbons in a parallel manner, such as cross-coupling of alkyl electrophiles[3–6], are highly valuable for drug development. However, the enantioselective cross-coupling of alkyl electrophiles, especially alkyl–alkyl coupling, remains challenging[3,4,7,8].

One strategy for enantioselective C(sp^3)–C(sp^3) coupling consists of enantioselective metal hydride addition to an internal olefin to form a chiral metal–alkyl intermediate, followed by enantiospecific alkyl–alkyl coupling (Fig. 1a). This approach creates a stereogenic centre at a carbon centre of the olefin and complements the enantioconvergent alkyl–alkyl coupling of racemic alkyl electrophiles[9–16], which is still limited in scope. Whereas reports of the stereoconvergent coupling of racemic α-zincated *N*-Boc-pyrrolidines with alkyl halides have suggested the feasibility of this mode of alkyl–alkyl coupling[17,18], the challenge rests on the ability of a metal hydride catalyst to perform both enantioselective addition to an internal olefin and coupling with non-activated alkyl electrophiles. The Cu–H-catalysed enantioselective functionalization of internal olefins has advanced rapidly in recent years[19–25], but the coupling of the in-situ-generated chiral organocopper intermediates with non-activated alkyl electrophiles remains elusive (Fig. 1b). For coupling with alkyl electrophiles, Ni–H catalysis is better suited than Cu–H catalysis[15,16,26,27]; however, Ni–H insertion into an internal olefin typically leads to chain walking to form a terminal, primary-alkyl–nickel intermediate[28–33], removing the chirality generated in the initial insertion (Fig. 1c).

An α-aryl or α-boryl directing group can stabilize a branched organonickel intermediate[27,34–36]. The enantioselective coupling of such an intermediate with an alkyl electrophile has remained elusive, although a single example of analogous coupling with PhI with low enantioselectivity (62% e.e.) has been reported[36]. Here, we describe the Ni–H-catalysed enantioselective C(sp^3)–C(sp^3) cross-coupling of non-activated alkyl halides with alkenyl boronates (Fig. 1d). This coupling yields a diverse range of chiral alkyl boronic acid pinacol esters (Bpins), which are both versatile intermediates and important endpoints to bio-active molecules[37–41]. Chiral alkyl boronates can be prepared by hydroboration[42], Matteson reaction[43] or using enantioenriched α-lithiated benzoates[44]. However, these strategies either suffer from regioselectivity issues or require stoichiometric amounts of chiral reagents. Recently, new approaches based on asymmetric catalysis such as hydrogenation[45], directed hydroboration[46], 1,2-metallate rearrangement[47] and enantioconvergent Negishi coupling[48] have been developed (Fig. 1e). Nevertheless, many limitations still exist. For example, specialized and hard-to-access substrates were required for hydrogenation, and substrates with a specific directing group were necessary for hydroboration. On the other hand, methods based on 1,2-metallate rearrangement and Negishi coupling employ reactive organometallic reagents, which compromise functional-group compatibility. By using readily available and stable olefins as nucleophiles and unactivated alkyl halides as electrophiles under mild reaction conditions, our method provides notable advantages in reaction efficiency, substrate availability and scope, as well as functional-group tolerance. In particular, applications for the post-product functionalization of many drug molecules and natural products are demonstrated.

Results and discussion

Reaction development. We recently developed the Ni–H-catalysed hydrocarbonation of alkenyl Bpins[27]. To achieve enantioselective C(sp^3)–C(sp^3) coupling based on this racemic reaction, we screened various chiral ligands and fine-tuned other reaction parameters. Our model reaction was the coupling of *trans*-1-hexenylboronic acid pinacol ester (**1a**) with 3-phenylpropyl iodide (**2a**) to give (*S*)-4,4,5,5-tetramethyl-2-(1-phenylnonan-4-yl)-1,3,2-dioxaborolane (**3a**) (Table 1). The optimized reaction conditions were established as the following: $NiCl_2$ (15 mol%) as the nickel source, Bi-Ox **L6** (20 mol%) as the ligand, diethoxymethylsilane (DEMS, 2.5 equiv.)

[1]Laboratory of Inorganic Synthesis and Catalysis, Institute of Chemical Sciences and Engineering, École Polytechnique Fédérale de Lausanne (EPFL), ISIC-LSCI, Lausanne, Switzerland. [2]These authors contributed equally: Srikrishna Bera and Runze Mao. ✉e-mail: xile.hu@epfl.ch

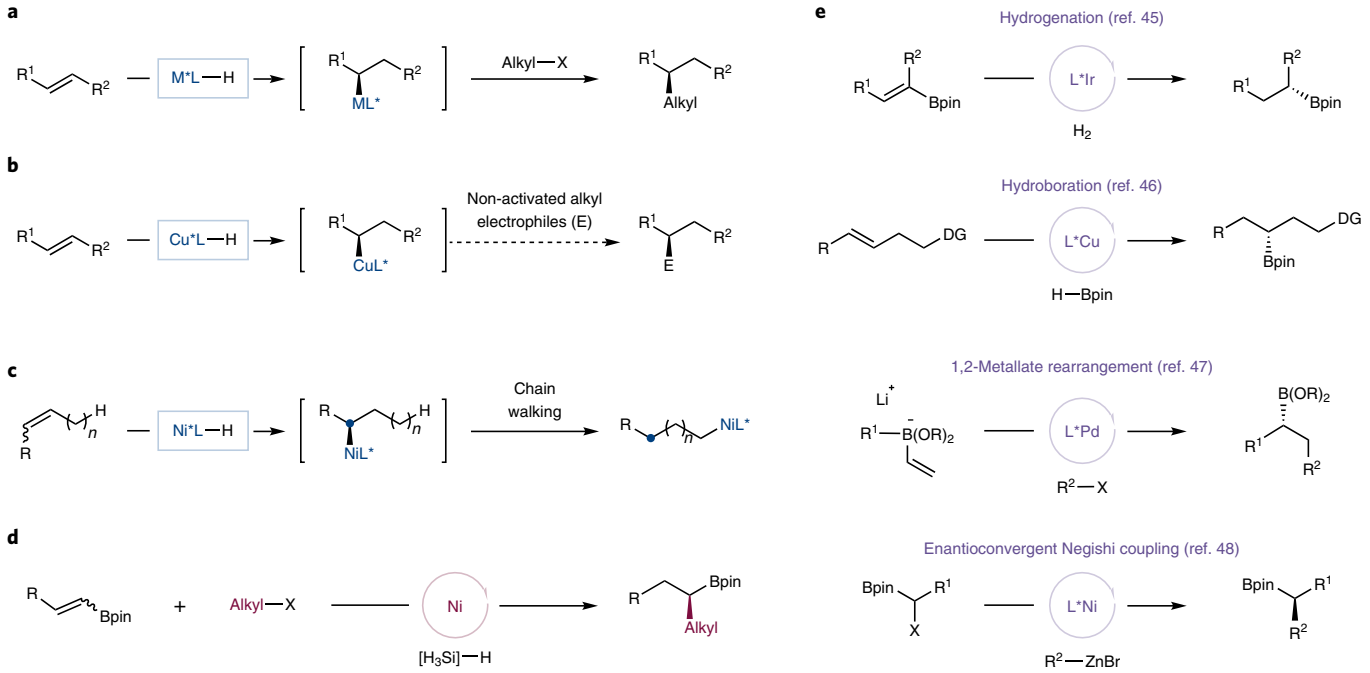

Fig. 1 | Strategies for enantioselective C(sp^3)–C(sp^3) cross-coupling. a, Enantioselective metal hydride insertion to internal olefins followed by enantiospecific alkyl–alkyl coupling. **b**, Challenge for Cu–H chemistry: no precedent for cross-coupling of non-activated alkyl electrophiles with a transient chiral alkyl–Cu intermediate. **c**, Challenge for Ni–H chemistry: an unwanted chain-walking event results in removal of the newly generated stereocentre (initially a new stereocentre is created upon metal hydride insertion into an olefin, but the stereocentre is lost due to chain walking generating a primary-alkyl–Ni species). **d**, This work: Ni-catalysed enantioselective cross-coupling of non-activated alkyl halides with internal olefins. **e**, Comparison to other catalytic methods for the synthesis of chiral alkyl boronates: asymmetric hydrogenation of specialized and hard-to-access substrates by iridium catalysis, asymmetric hydroboration of olefins bearing a specific directing group by copper catalysis, Pd-catalysed asymmetric 1,2-metallate rearrangement followed by cross-coupling, which employs highly reactive and difficult-to-handle organolithium (RLi) reagents, and Ni-catalysed enantioconvergent cross-coupling of α-halo boronates with highly reactive organozinc (RZnBr) reagents. These methods provide limited substrate scope and were less practical or general than the method described in the current work. DG, directing group.

as the hydride source, KF (2.5 equiv.) as the base, a 3:2 mixture of 1,2-dichloroethane and dimethylformamide (DCE–DMF) as the solvent, at room temperature, and a 40 h reaction time. Under these conditions, **3a** was obtained as a single regioisomer in 72% gas chromatographic yield (69% isolated yield) and 92% e.e. (entry 1, Table 1). The main side products were an alkane originated from protodeiodination of **2a** and an alkyl chloride originated from transhalogenation of **2a** with $NiCl_2$. Products that would form due to Suzuki-type cross-coupling or hydrosilylation of alkenyl Bpin or HI elimination from alkyl iodide were not detected.

The influence of different reaction parameters in the outcome of the reaction is described in Supplementary Tables 1–6. A concise summary of key observations is shown in Table 1. Structurally related Pyr-Ox (**L1** and **L2**) and Box (**L3**) ligands were inefficient in this transformation (entries 2-4, Table 1). Bi-Ox ligands with alkyl substituents (**L4** and **L5**) gave lower yields or e.e. values (entries 5 and 6, Table 1). The reactions were sensitive to the substituents on the aryl units of the Bi-Ox ligands (see Supplementary Table 3). Other nickel(II) sources such as $NiBr_2$ and $NiBr_2$·diglyme afforded lower yields and enantioselectivities (entries 7 and 8, Table 1). The use of $Ni(COD)_2$ as a precatalyst led to a lower yield and e.e. (entry 9). Among alkali-metal fluoride bases, those containing a large cation (that is, Rb^+ and Cs^+) gave good yields while those with a small cation (that is, Li^+ and Na^+) shut down the hydroalkylation (see Supplementary Table 6)[49]. Compared with KF, CsF and RbF decreased the enantioselectivity (entry 10, Table 1 and see Supplementary Table 6)[50]. We suspect that a non-covalent interaction network between the alkali-metal cation, the π-system of the phenyl unit of **L6** and the oxygen atom of the boronic ester was important for the enantioselectivity, which is then sensitive to the nature of the cation[51,52]. Reactions were sensitive to the substituents of hydrosilanes (see Supplementary Table 5). Whereas a variety of hydrosiloxanes could be used, less electrophilic hydrosilanes such as Et_3SiH, $PhSiH_3$, Ph_3SiH and $PhMe_2SiH$ were inefficient hydride donors, probably because they could not be activated by KF to form a reactive penta-coordinate hydrosilicate species[53]. Reactions using DEMS, PMHS (polymethylhydrosiloxane) and $(EtO)_3SiH$ gave similar enantioselectivities, but the reaction using DEMS had the highest yield (entry 11, Table 1 and see Supplementary Table 5). A lower amount of DEMS (1.5 equiv.) diminished the yield (53%) but not the enantioselectivity, suggesting that a larger amount of DEMS was necessary to promote the formation and insertion of Ni–H against side reactions[54]. The mixed solvent (DCE–DMF) turned out as the best solvent to achieve high enantioselectivity. DCE alone was not a suitable solvent (entry 13, Table 1), likely because it cannot dissolve a sufficient amount of $NiCl_2$. The reaction in DMF alone had a similar yield but a lower e.e. than that in the mixed solvent (entry 12, Table 1), demonstrating a sensitivity of the enantioselectivity on the solvent properties. Using a pre-formed $NiCl_2$–**L6** complex as the catalyst gave the product in 61% yield with 92% e.e. (see Supplementary Information section 12.7), suggesting the presence of this species in the catalytic cycle.

Substrate scope. The scope of this enantioselective coupling method is broad (Table 2). In addition to an aryl group (**3a**, **3b** and **3j**), primary alkyl iodides containing a pendant ether (**3c**), ketone (**3d**), ester

Table 1 | Summary of the effects of reaction parameters on the reaction efficiency[a]

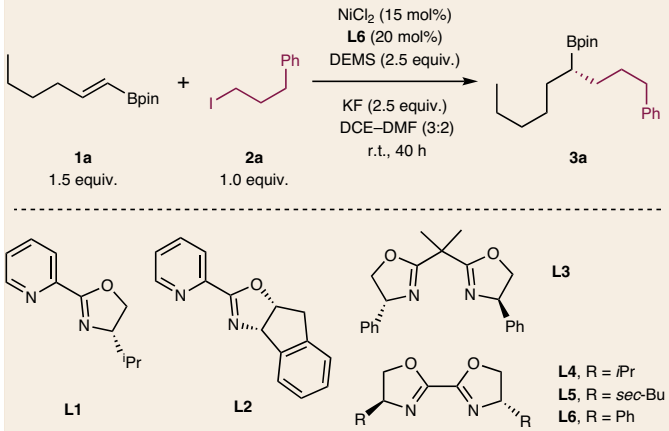

Entry	Variants	Yield (%)	e.e. (%)[b]
1	None	72 (69)[c]	92
2	**L1**	73	52
3	**L2**	76	42
4	**L3**	31	36[d]
5	**L4**	47	60
6	**L5**	37	58
7	$NiBr_2$	52	80
8	$NiBr_2$·diglyme	51	84
9	$Ni(COD)_2$	31	80
10[e]	CsF	70	68
11	PMHS	57	91
12	DMF as solvent	73	66
13	DCE as solvent	n.d.	n.d.

[a]See Supplementary Information section 2 for experimental details; all reactions were carried out in a 0.1 mmol scale with respect to **2a**; corrected gas chromatographic yields using *n*-dodecane as an internal standard were reported. [b]Determined using HPLC analysis of the corresponding alcohol after stereospecific oxidation of the boronic ester (see Supplementary Information section 2 for full details). [c]Isolated yield is shown in parentheses. [d]The opposite enantiomer was enriched. [e]Reaction time = 12 h. COD, 1,5-cyclooctadiene; n.d., not detected.

(**3e**, **3f**, **3k** and **3l**), carbamate (**3h**), phthalimide (**3i**) and amine (**3m** and **3n**) groups all reacted well. These data rule out the possibility of a specific group that directs the enantioselectivity of the coupling. A high level of functional-group tolerance, unusual for cross-coupling of organometallic reagents, was achieved. For example, an unprotected OH group was compatible (**3j**). Despite the ability of nickel to activate aryl iodides, bromides and chlorides, our method tolerated these potentially reactive groups (**3e**–**3g**). Substrates containing medicinally relevant heterocycles such as furan (**3k**), thiophene (**3l**), indole (**3m**) and piperidine (**3n**) were also viable.

The coupling of alkyl bromides required an in situ Br/I exchange and was slightly less efficient than the corresponding coupling of alkyl iodides. For example, the coupling of *trans*-1-hexenylboronic acid pinacol ester (**1a**) with 3-phenylpropyl bromide gave **3a** in 50% yield and 86% e.e. in the presence of 40 mol% KI. By comparison, an analogous coupling using the corresponding alkyl iodide **2a** gave 69% yield and 92% e.e. Similar yields and e.e. values were obtained for two other alkyl bromides (**3o** and **3p**). More inert alkyl electrophiles such as alkyl chloride or alkyl triflate were unsuitable coupling partners. Coupling of an alkyl triflate in the presence of 40 mol% KI gave only a trace amount of the desired product, indicating the inefficiency of triflate/I exchange.

The enantioselective cross-coupling of two secondary alkyl fragments is challenging[55]. Thus, it is noteworthy that the present method also works for the coupling of secondary alkyl iodides, including both acyclic and cyclic substrates, delivering the corresponding alkyl Bpins with good yields and high enantioselectivity (**4a**–**4i**). Medicinally interesting cyclic groups such as indane, oxetane and azeditine were tolerated (**4d**–**4i**). No isomerization was observed in the alkyl fragments. Coupling of unsymmetrical secondary alkyl iodides gave good yields, but no diastereoselectivity (**4j**–**4l**). The enantioselectivities for both diastereomers were high (90–95% e.e.). The coupling of unactivated tertiary alkyl iodides such as *tert*-butyl iodide and 1-iodoadamentane was unsuccessful (for example, **4m**), likely due to steric hindrance against oxidative addition of the iodide to Ni.

A wide range of alkenyl Bpins could be used as nucleophiles to deliver the corresponding enantiomerically enriched alkyl Bpins (**5a**–**5i**) (Table 2). The coupling was regioselective at the carbon α- to the Bpin group. The alkenes can contain functional groups such as alkyl chloride (**5a**), ester (**5b** and **5c**) and ether (**5d**, **5e** and **5f**). Vinylboronate, a synthetically useful substrate posing a challenge in regioselectivity, was coupled in high enantioselectivity (90% e.e.) and regioselectivity (12:1 branched:linear). Coupling of a sterically demanding β,β′-disubstituted alkenyl Bpin was less efficient, giving the product in 30% yield. Coupling of a trisubstituted vinyl boronate 2-(cyclohex-1-en-1-yl)-4,4,5,5-tetramethyl-1,3,2-dioxaborolane was unsuccessful, probably due to difficulty in the addition of Ni–H to the olefin compared with protodeiodination of the alkyl iodide. Among the organoboron reagents, Bpin derivatives seem unique for this transformation. The coupling of the alkenyl 9-borabicyclo[3.3.1]nonane (9-BBN) derivative of boronic acid was unsuccessful as this reagent seemed to decompose under the reaction conditions. Using this type of reagent, the majority of alkyl iodides remained intact.

The Bpin groups in products **3e** and **4g** were stereospecifically oxidized to give alcohols (**3e**′ and **4g**′; see Supplementary Information section 14). The X-ray crystal structures of **3e**′ and **4g**′ revealed the absolute configuration of the chiral carbon centres. By analogy, we assigned the corresponding absolute configurations to all products.

The reaction of a *cis*-alkenyl Bpin (**1l**) gave a product (**3b**) identical to the reaction of its *trans*-analogue (see Supplementary Information section 12.1). However, under the reaction conditions specified and even without a Ni catalyst, *cis*-alkenyl Bpin (**1l**) would first be converted to its *trans*-analogue (**1a**) prior to hydroalkylation (see Supplementary Information section 12.2).

Synthetic applications and diversification of chiral products. The functionalization of drug molecules and natural products typically requires mild reaction conditions and high functional-group tolerance. As such, the present method is well suited for this purpose, and it could be used for synthesizing an array of chiral alkyl Bpins bearing complex or bio-active alkyl fragments derived from drugs and natural products (Table 3). Alkyl iodides bearing multiple stereocentres, such as **6a**, a chiral terpinol derived from nopol; naproxen (**6b**), a non-steroidal anti-inflammatory drug; and lithocholic acid derivative **6d**, were all viable electrophiles that yielded potentially valuable products in synthetically useful yields and with high diastereoselectivity. In addition, alkyl iodides derived from drugs such as gemfibrozil (**6c**), isoxepac (**6f**), indomethacin (**6g**), probenecid (**6h**) and adapalene (**6i**) as well as from herbicide 2,4-D (**6e**) were transformed into the corresponding chiral alkyl Bpins with ease.

Chiral alkyl Bpins are powerful intermediates in asymmetric organic synthesis because the C–B moiety can be easily transformed into a C–X moiety (X = C or heteroatom) with the conservation of chirality at the α-C centre[39,40]. We provide several illustrative examples in Fig. 2a for the transformation of one coupling

Table 2 | Scope of Ni–H-catalysed enantioselective C(sp^3)–C(sp^3) coupling[a]

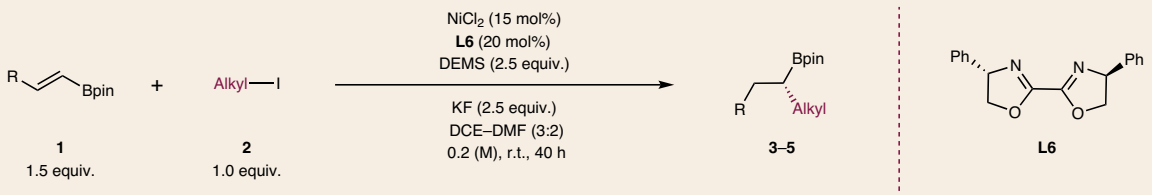

1 1.5 equiv. **2** 1.0 equiv. **3–5** **L6**

Primary alkyl iodides

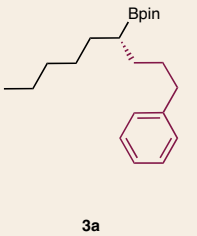

3a 69%, 92% e.e. 50%, 86% e.e.[b]

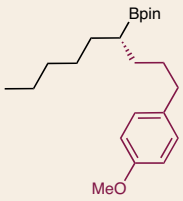

3b 80%, 90% e.e.

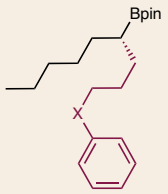

3c, X = O, 72%, 89% e.e. **3d**, X = C=O, 67%, 92% e.e.

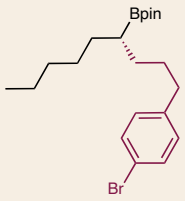

3e 73%, 89% e.e.[c]

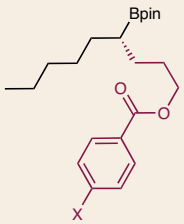

3f, X = Cl, 64%, 90% e.e. **3g**, X = I, 46%, 90% e.e.[c]

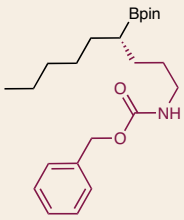

3h 70%, 88% e.e.

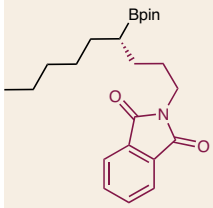

3i 75%, 90% e.e.

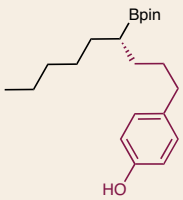

3j 55%, 93% e.e.

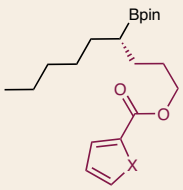

3k, X = O,71%, 90% e.e. **3l**, X = S, 60%, 90% e.e.

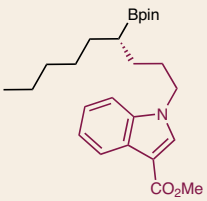

3m 50%, 91% e.e.

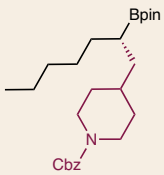

3n 79%, 92% e.e.

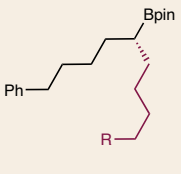

3o, R = CO_2Me, 54%, 83% e.e. **3p**, R = OPh, 54%, 85% e.e. From alkyl bromides[b,c,d]

Secondary and tertiary alkyl iodides[c]

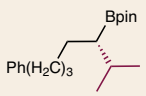

4a 70%, 93% e.e.

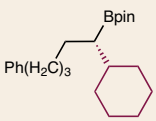

4b 67%, 93% e.e.

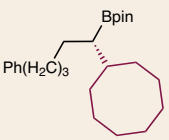

4c 78%, 90% e.e.

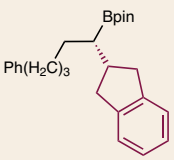

4d 69%, 91% e.e.

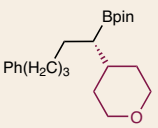

4e 70%, 92% e.e.

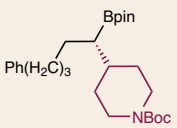

4f 61%, 92% e.e.

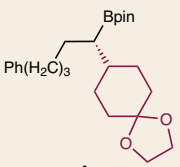

4g 63%, 92% e.e.

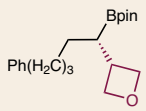

4h 58%, 85% e.e.

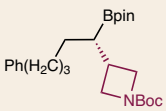

4i 51%, 89% e.e.

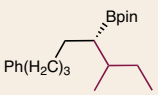

4j 70%, 1:1.04 d.r. 94% e.e., 95% e.e.

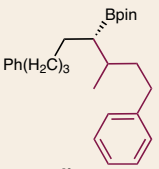

4k 69%, 1:1.05 d.r. 94% e.e., 94% e.e.

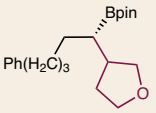

4l 75%, 1:1.1 d.r. 90% e.e., 90% e.e.

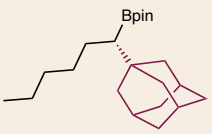

4m <5%, n.d. From tertiary alkyl iodide

Alkenyl boronates

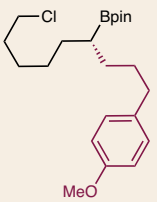

5a 61%, 91% e.e.

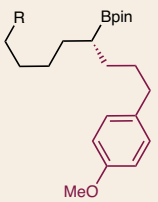

5b (R = CO_2Me), 57%, 90% e.e. **5c** (R = OAc), 77%, 91% e.e. **5d** (R = CH_2OPh), 69%, 90% e.e.

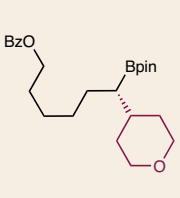

5e 79%, 90% e.e.[c]

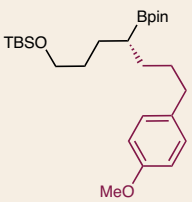

5f 56%, 92% e.e.

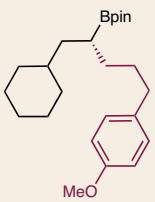

5g 54%, 91% e.e.

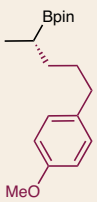

5h 68%, 90% e.e.[e]

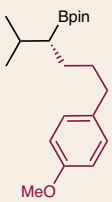

5i 30%, 91% e.e.[e]

[a]Conditions: all reactions were carried out with $NiCl_2$ (15 mol%), ligand **L12** (20 mol%), **1** (0.15 mmol), **2** (0.10 mmol), DEMS (0.25 mmol), KF (0.25 mmol) and DCE–DMF (0.5 ml) at room temperature for 40 h. Enantiomeric excess (e.e.) values were determined using HPLC analysis (see Supplementary Information section 6 for full details). [b]Alkyl bromide with 40 mol% KI was used. [c]Compounds **1** (0.1 mmol) and **2** (0.15 mmol) were used. [d]Reactions were conducted on a 0.2 mmol scale with respect to **1**. [e]Reactions were conducted on a 0.2 mmol scale with respect to **2**. BzO, benzoyl; TBS, *t*-butyldimethylsilyl.

Table 3 | Functionalization of natural product and drug derivatives[a]

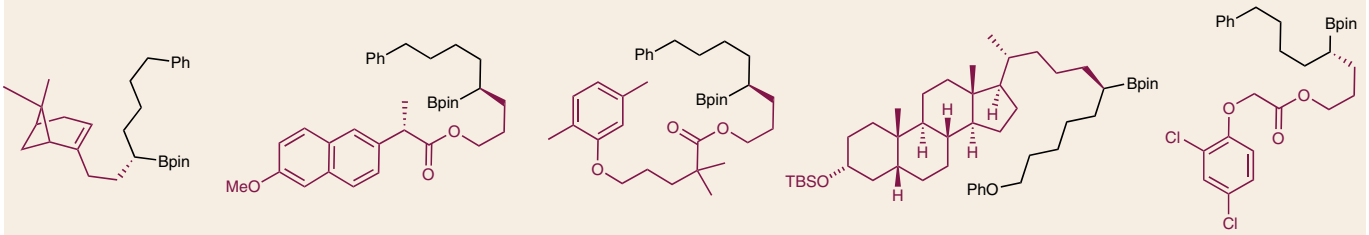

6a (55%, 95:5 d.r.)
From nopol

6b (68%, 94:6 d.r.)
From naproxen

6c (57%, 91% e.e.)
From gemfibrozil

6d (43%, 95:5 d.r.)
From lithocholic acid

6e (64%, 89% e.e.)
From 2,4-D

6f (58%, 92% e.e.)
From isoxepac

6g (53%, 90% e.e.)
From indomethacin

6h (60%, 89% e.e.)
From probenecid

6i (59%, 90% e.e.)
From adapalene

[a]Conditions: all reactions were carried out with $NiCl_2$ (15 mol%), ligand **L12** (20 mol%), **1** (0.15 mmol), **2** (0.10 mmol), DEMS (0.25 mmol), KF (0.25 mmol) and DCE–DMF (0.5 ml) at room temperature for 40 h. Enantiomeric excess (e.e.) and diastereomeric ratio (d.r.) values were determined using HPLC analysis (see Supplementary Information section 6 for full details).

product **4e**. C–C, C–O and C–Br bond-formation reactions proceeded cleanly, affording chiral organic compounds (**7**–**10**) without erosion in enantiomeric excess. We also applied our method for the enantioselective synthesis of a key chiral amino alcohol intermediate to the drug (*S*)-(+)-pregabalin (Fig. 2b)[56]. Coupling of *trans*-3-methyl-1-butenyl boronic acid pinacol ester (**1m**) with *tert*-butyl(2-iodoethoxy)diphenylsilane (**2m′**) provided **11** in 42% yield with 90% e.e. Stereospecific homologation of **11**, amination and silyl ether-deprotection provided the amino alcohol intermediate **12** in 43% overall yield from **11**. Then, conversion of **12** to pregabalin, which has been previously reported[57]. A gram-scale reaction between *trans*-5-phenyl-1-pentenyl boronic acid pinacol ester (**1b**) and 4-iodotetrahydro-2*H*-pyran (**2v**) using a reduced catalyst loading (10 mol%) afforded **4e** in 62% yield (1.116 g) and 93% e.e. (Fig. 2c). A one-pot reaction sequence consisted of the hydroboration of 1-hexyne to give alkenyl Bpin **1a** in situ, followed by cross-coupling with **2b** without isolating **1a**, to yield **3b** in 74% yield and 90% e.e. (Fig. 2d). These results further showcase the preparative utility of the coupling.

Mechanistic considerations. When radical clock 5-hexenyliodide (**2n′**) was used as a substate, cyclization occurred. The product (**13**) originated from cyclization of the 5-hexenyl radical and was obtained in 11% yield and 91% e.e. (Fig. 3a). The coupling product that originated from the uncyclized 5-hexenyl radical was also detected but it was difficult to purify and isolate. These data support the intermediacy of alkyl radicals. For example, when 1.0 equiv. of radical scavenger (2,2,6,6-tetramethylpiperidin-1-yl)oxyl (TEMPO) was added to the reaction, no desired product was detected (Fig. 3b).

The regioselectivity of the reactions might be due to two factors: (1) stabilization of the α-boryl Ni–alkyl intermediate by the vacant *p* orbital of the Bpin unit. Similar regioselectivity was observed in the addition of Cp_2ZrHCl (Schwartz's reagent) to alkenyl BBN[58]. (2) Coordination of the oxygen atom of the Bpin unit to the Ni centre. We tested the second possibility using a tridentate Py-box ligand (**L20**), which was expected to hamper the coordination of the oxygen atom of the Bpin to the nickel centre. Although the coupling yield was modest (31%), the reaction is highly α-selective (r.r. = 13:1) (Fig. 3c). This result suggests that the regioselectivity is not likely due to oxygen coordination.

We tested several substrates (**1n**, **1o** and **1p**) where the alkenyl group is distal to the Bpin group (Fig. 3d). Products originating from hydroalkylation at the α-C to Bpin were obtained in low to modest yields but with high enantioselectivity (90% and above). Other regioisomers were also formed. These data indicate chain walking of the distal alkenyl group mediated by Ni–H until the stable α-boryl Ni-alkyl species is formed.

The mechanism of this Ni–H-catalysed enantioselective C(sp^3)–C(sp^3) cross-coupling is proposed in Fig. 3e, analogous to a previous proposal on Ni-catalysed hydroalkylation[15]. Under the reaction conditions, a chiral L*Ni$^{(I)}$–Cl species (**A**) is formed as the actual catalyst, which undergoes single electron transfer with an alkyl iodide to generate an alkyl radical and L*ClNi$^{(II)}$–I (**B**). The reaction of **B** with a hydrosilane generates the Ni–H species L*ClNi$^{(II)}$–H (**C**) which inserts to alkenyl Bpin. The insertion is regioselective at the α-C to the boryl group, generating a chiral alkyl intermediate (**D**). The resulting Ni–alkyl intermediate (**D**) then recombines with the alkyl radical to give a high-valent Ni(III) complex (**E**), which undergoes reductive elimination to give the product. We propose that the stereoselective step is the insertion of a chiral Ni–H into the olefin. Alternatively, the reaction proceeds by reversible Ni-alkyl homolysis followed by stereoselective reductive elimination[59]. The reaction profile excludes a kinetic-resolution process (see Supplementary Information section 12.3).

Conclusion

In summary, we have developed a Ni–H-catalysed enantioselective C(sp^3)–C(sp^3) coupling of non-activated alkyl iodides with alkenyl Bpins. By employing readily available and stable olefins as nucleophiles, this coupling enables the streamlined synthesis of chiral alkyl Bpins under mild conditions, with a previously unattained scope and functional-group tolerance. Examples in post-product

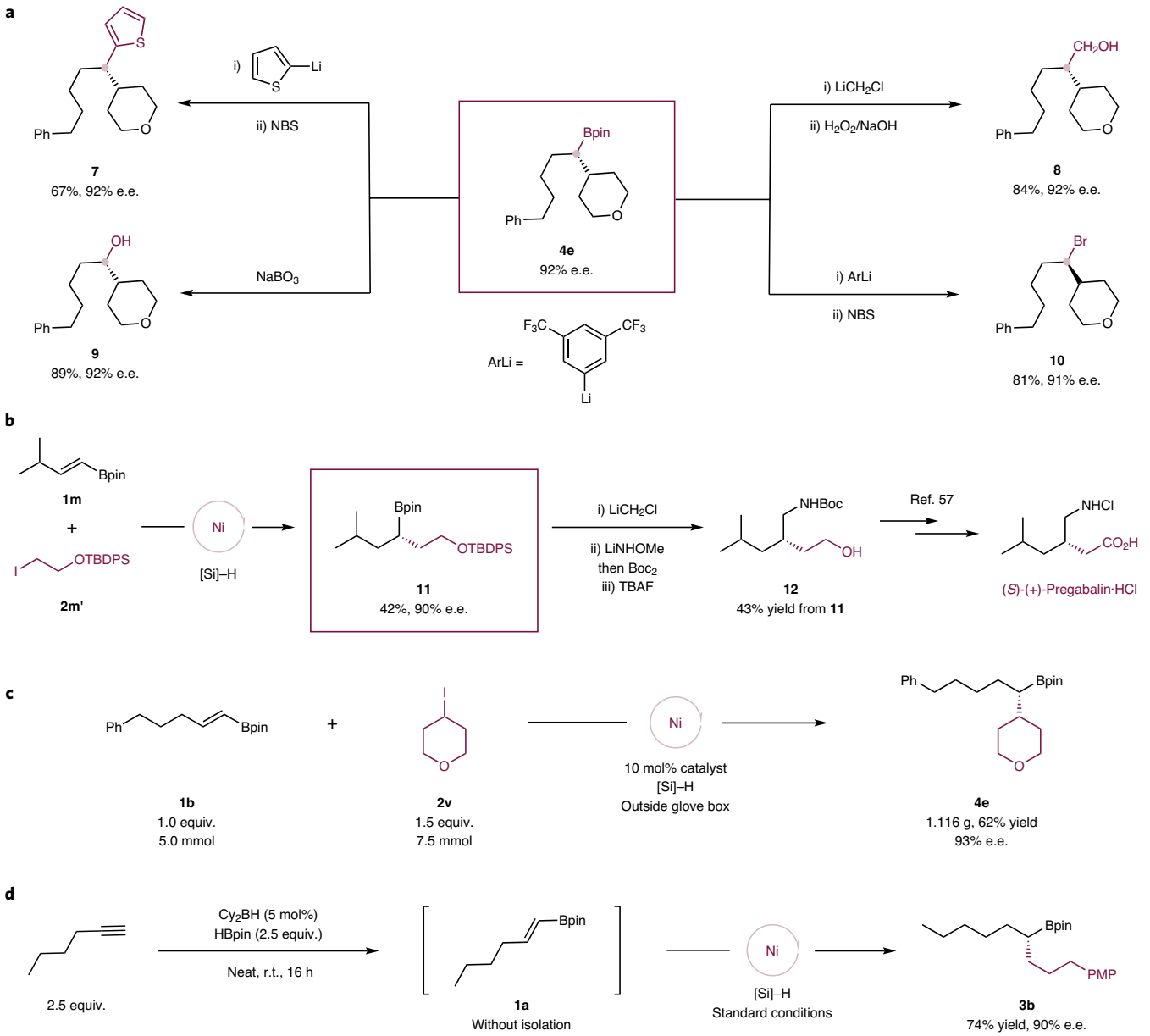

Fig. 2 | Synthetic applications. a, Conversion of chiral alkyl Bpins to a diverse array of valuable chiral products such as C–heteroarene coupling product **7**, homologation followed by oxidation to a primary alcohol bearing a β-tertiary carbon stereocentre **8**, alcohol **9** through oxidation and alkyl bromide **10** via C–Br bond formation (see Supplementary Information section 7 for full details). **b**, Synthesis of **12**, a key intermediate of (*S*)-(+)-pregabalin (see Supplementary Information section 8 for full details). **c**, A gram-scale reaction using 10 mol% catalyst (see Supplementary Information section 10 for full details). **d**, One-pot asymmetric hydroalkylation without isolation of alkenyl Bpin (see Supplementary Information section 11 for full details). NBS, *N*-bromosuccinimide; TBDPS, *tert*-butyldiphenylsilyl; TBAF, tetrabutylammonium fluoride; PMP, *para*-methoxyphenyl.

functionalization and chiral syntheses demonstrate the potential utility of this method in drug discovery.

Online content

Any methods, additional references, Nature Research reporting summaries, source data, extended data, supplementary information, acknowledgements, peer review information; details of author contributions and competing interests; and statements of data and code availability are available at https://doi.org/10.1038/s41557-020-00576-z.

Received: 14 January 2020; Accepted: 12 October 2020;
Published online: 30 December 2020

References

1. Lovering, F., Bikker, J. & Humblet, C. Escape from flatland: increasing saturation as an approach to improving clinical success. *J. Med. Chem.* **52**, 6752–6756 (2009).
2. Ritchie, T. J. & Macdonald, S. J. The impact of aromatic ring count on compound developability – are too many aromatic rings a liability in drug design? *Drug Discov. Today* **14**, 1011–1020 (2009).
3. Choi, J. & Fu, G. C. Transition metal-catalyzed alkyl–alkyl bond formation: another dimension in cross-coupling chemistry. *Science* **356**, eaaf7230 (2017).
4. Fu, G. C. Transition-metal catalysis of nucleophilic substitution reactions: a radical alternative to S_N1 and S_N2 processes. *ACS Cent. Sci.* **3**, 692–700 (2017).
5. Hu, X. Nickel-catalyzed cross coupling of non-activated alkyl halides: a mechanistic perspective. *Chem. Sci.* **2**, 1867–1886 (2011).
6. Rudolph, A. & Lautens, M. Secondary alkyl halides in transition-metal-catalyzed cross-coupling reactions. *Angew. Chem. Int. Ed.* **48**, 2656–2670 (2009).

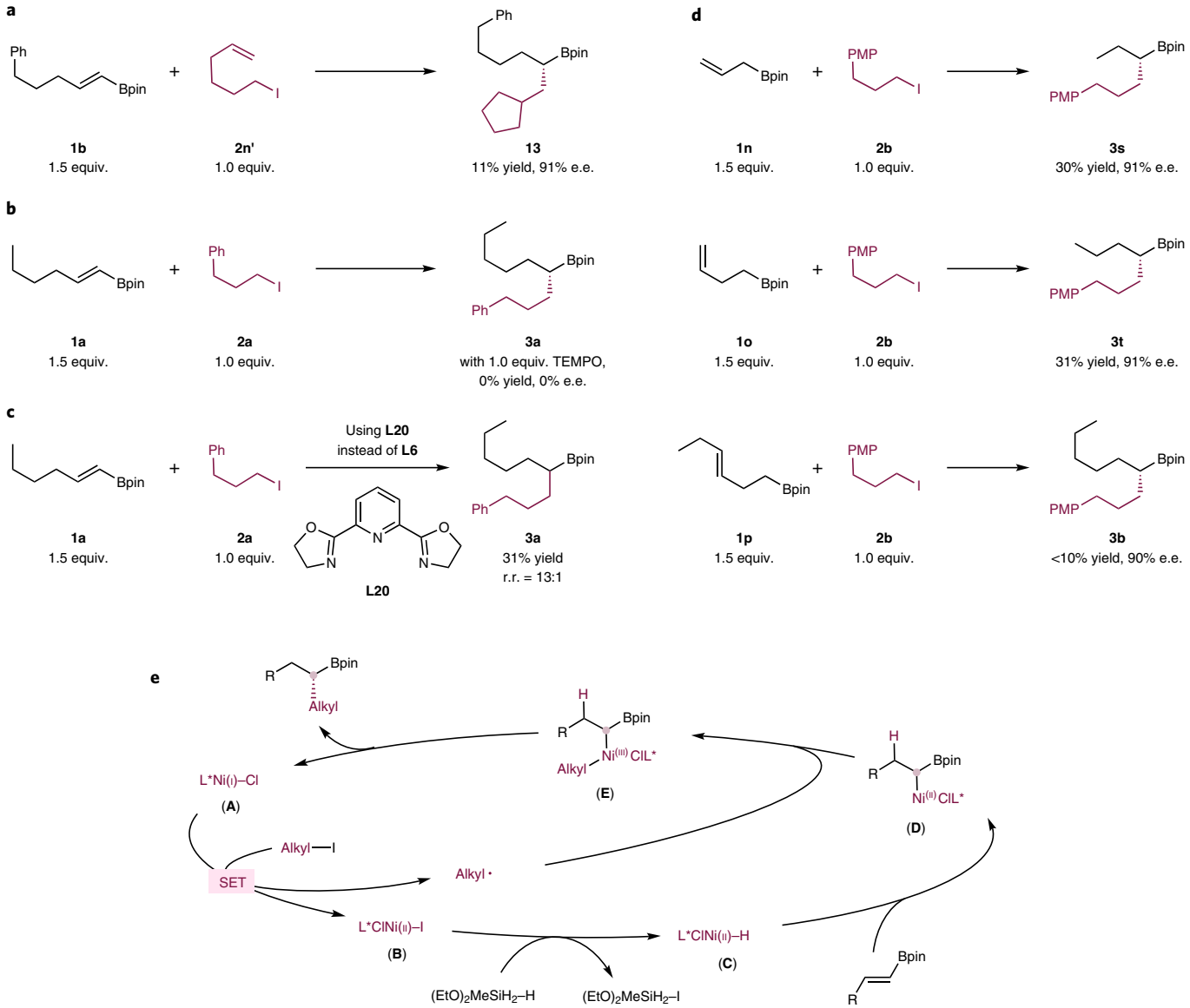

Fig. 3 | Mechanistic studies of the catalytic enantioselective C(sp^3)–C(sp^3) cross-coupling. a, Radical-clock experiment with alkene-tethered alkyl iodide **2n**′ afforded the formation of **13** under standard conditions, suggesting the intermediacy of an alkyl radical and its subsequent cyclization and C(sp^3)–C(sp^3) coupling (see Supplementary Information section 12.4 for full details). **b**, The reaction was completely shut down by the addition of radical scavanger TEMPO (see Supplementary Information section 12.5 for full details). **c**, Probe for origin of regioselectivity using a tridentate Py-box ligand (**L20**) instead of **L6** (see Supplementary Information section 12.6 for full details); r.r., regioisomeric ratio. **d**, Reactions with substrates where the alkenyl group is distal to the Bpin group: chain-walking products were formed with high enantioselectivity under standard conditions (see Supplementary Information section 13 for full details). **e**, Outline of possible reaction pathway for Ni-catalysed enantioselective C(sp^3)–C(sp^3) cross-coupling. SET, single electron transfer.

7. Cherney, A. H., Kadunce, N. T. & Reisman, S. E. Enantioselective and enantiospecific transition-metal-catalyzed cross-coupling reactions of organometallic reagents to construct C–C bonds. *Chem. Rev.* **115**, 9587–9652 (2015).
8. Glasspoole, B. W. & Crudden, C. M. The final frontier. *Nat. Chem.* **3**, 912–913 (2011).
9. Owston, N. A. & Fu, G. C. Asymmetric alkyl–alkyl cross-couplings of unactivated secondary alkyl electrophiles: stereoconvergent Suzuki reactions of racemic acylated halohydrins. *J. Am. Chem. Soc.* **132**, 11908–11909 (2010).
10. Wilsily, A., Tramutola, F., Owston, N. A. & Fu, G. C. New directing groups for metal-catalyzed asymmetric carbon–carbon bond-forming processes: stereoconvergent alkyl–alkyl Suzuki cross-couplings of unactivated electrophiles. *J. Am. Chem. Soc.* **134**, 5794–5797 (2012).
11. Zultanski, S. L. & Fu, G. C. Catalytic asymmetric γ-alkylation of carbonyl compounds via stereoconvergent Suzuki cross-couplings. *J. Am. Chem. Soc.* **133**, 15362–15364 (2011).
12. Arp, F. O. & Fu, G. C. Catalytic enantioselective Negishi reactions of racemic secondary benzylic halides. *J. Am. Chem. Soc.* **127**, 10482–10483 (2005).
13. Fischer, C. & Fu, G. C. Asymmetric nickel-catalyzed Negishi cross-couplings of secondary α-bromo amides with organozinc reagents. *J. Am. Chem. Soc.* **127**, 4594–4595 (2005).
14. Son, S. & Fu, G. C. Nickel-catalyzed asymmetric Negishi cross-couplings of secondary allylic chlorides with alkylzincs. *J. Am. Chem. Soc.* **130**, 2756–2757 (2008).
15. Wang, Z., Yin, H. & Fu, G. C. Catalytic enantioconvergent coupling of secondary and tertiary electrophiles with olefins. *Nature* **563**, 379–383 (2018).
16. Zhou, F., Zhang, Y., Xu, X. & Zhu, S. NiH-catalyzed remote asymmetric hydroalkylation of alkenes with racemic α-bromo amides. *Angew. Chem. Int. Ed.* **58**, 1754–1758 (2019).
17. Cordier, C. J., Lundgren, R. J. & Fu, G. C. Enantioconvergent cross-couplings of racemic alkylmetal reagents with unactivated secondary alkyl electrophiles: catalytic asymmetric Negishi α-alkylations of *N*-Boc-pyrrolidine. *J. Am. Chem. Soc.* **135**, 10946–10949 (2013).

18. Mu, X., Shibata, Y., Makida, Y. & Fu, G. C. Control of vicinal stereocenters through nickel-catalyzed alkyl–alkyl cross-coupling. *Angew. Chem. Int. Ed.* **56**, 5821–5824 (2017).
19. Deutsch, C., Krause, N. & Lipshutz, B. H. CuH-catalyzed reactions. *Chem. Rev.* **108**, 2916–2927 (2008).
20. Pirnot, M. T., Wang, Y. M. & Buchwald, S. L. Copper hydride catalyzed hydroamination of alkenes and alkynes. *Angew. Chem. Int. Ed.* **55**, 48–57 (2016).
21. Zhu, S., Niljianskul, N. & Buchwald, S. L. Enantio- and regioselective CuH-catalyzed hydroamination of alkenes. *J. Am. Chem. Soc.* **135**, 15746–15749 (2013).
22. Miki, Y., Hirano, K., Satoh, T. & Miura, M. Copper-catalyzed intermolecular regioselective hydroamination of styrenes with polymethylhydrosiloxane and hydroxylamines. *Angew. Chem. Int. Ed.* **52**, 10830–10834 (2013).
23. Wang, Y. M., Bruno, N. C., Placeres, A. L., Zhu, S. & Buchwald, S. L. Enantioselective synthesis of carbo- and heterocycles through a CuH-catalyzed hydroalkylation approach. *J. Am. Chem. Soc.* **137**, 10524–10527 (2015).
24. Yang, Y., Perry, I. B. & Buchwald, S. L. Copper-catalyzed enantioselective addition of styrene-derived nucleophiles to imines enabled by ligand-controlled chemoselective hydrocupration. *J. Am. Chem. Soc.* **138**, 9787–9790 (2016).
25. Bandar, J. S., Ascic, E. & Buchwald, S. L. Enantioselective CuH-catalyzed reductive coupling of aryl alkenes and activated carboxylic acids. *J. Am. Chem. Soc.* **138**, 5821–5824 (2016).
26. Lu, X. et al. Practical carbon–carbon bond formation from olefins through nickel-catalyzed reductive olefin hydrocarbonation. *Nat. Commun.* **7**, 11129 (2016).
27. Bera, S. & Hu, X. Nickel-catalyzed regioselective hydroalkylation and hydroarylation of alkenyl boronic esters. *Angew. Chem. Int. Ed.* **58**, 13854–13859 (2019).
28. Buslov, I., Becouse, J., Mazza, S., Montandon-Clerc, M. & Hu, X. Chemoselective alkene hydrosilylation catalyzed by nickel pincer complexes. *Angew. Chem. Int. Ed.* **54**, 14523–14526 (2015).
29. Gaydou, M., Moragas, T., Juliá-Hernández, F. & Martin, R. Site-selective catalytic carboxylation of unsaturated hydrocarbons with CO_2 and water. *J. Am. Chem. Soc.* **139**, 12161–12164 (2017).
30. Zhou, F., Zhu, J., Zhang, Y. & Zhu, S. NiH-catalyzed reductive relay hydroalkylation: a strategy for the remote C(sp^3)–H alkylation of alkenes. *Angew. Chem. Int. Ed.* **57**, 4058–4062 (2018).
31. Sommer, H., Juliá-Hernández, F., Martin, R. & Marek, I. Walking metals for remote functionalization. *ACS Cent. Sci.* **4**, 153–165 (2018).
32. Sun, S.-Z., Börjesson, M., Martin-Montero, R. & Martin, R. Site-selective Ni-catalyzed reductive coupling of α-haloboranes with unactivated olefins. *J. Am. Chem. Soc.* **140**, 12765–12769 (2018).
33. Sun, S.-Z., Romano, C. & Martin, R. Site-selective catalytic deaminative alkylation of unactivated olefins. *J. Am. Chem. Soc.* **141**, 16197–16201 (2019).
34. He, Y., Cai, Y. & Zhu, S. Mild and regioselective benzylic C–H functionalization: Ni-catalyzed reductive arylation of remote and proximal olefins. *J. Am. Chem. Soc.* **139**, 1061–1064 (2017).
35. Vasseur, A., Bruffaerts, J. & Marek, I. Remote functionalization through alkene isomerization. *Nat. Chem.* **8**, 209–219 (2016).
36. Zhang, Y., Han, B. & Zhu, S. Rapid access to highly functionalized alkyl boronates by NiH-catalyzed remote hydroarylation of boron-containing alkenes. *Angew. Chem. Int. Ed.* **58**, 13860–13864 (2019).
37. Davidson, M., Hughes, A. K., Marder, T. B. & Wade, K. *Contemporary Boron Chemistry* (Royal Society of Chemistry, 2000).
38. Liu, S.-Y. & Stephan, D. W. Contemporary research in boron chemistry. *Chem. Soc. Rev.* **48**, 3434–3435 (2019).
39. Leonori, D. & Aggarwal, V. K. Stereospecific couplings of secondary and tertiary boronic esters. *Angew. Chem. Int. Ed.* **54**, 1082–1096 (2015).
40. Sandford, C. & Aggarwal, V. K. Stereospecific functionalizations and transformations of secondary and tertiary boronic esters. *Chem. Commun.* **53**, 5481–5494 (2017).
41. Collins, B. S. L., Wilson, C. M., Myers, E. L. & Aggarwal, V. K. Asymmetric synthesis of secondary and tertiary boronic esters. *Angew. Chem. Int. Ed.* **56**, 11700–11733 (2017).
42. Brown, H. C. & Zweifel, G. Hydroboration as a convenient procedure for the asymmetric synthesis of alcohols of high optical purity. *J. Am. Chem. Soc.* **83**, 486–487 (1961).
43. Hall, D. G. (ed.) *Boronic Acids: Preparation, Applications in Organic Synthesis and Medicine* (Wiley–VCH, 2006).
44. Burns, M. et al. Assembly-line synthesis of organic molecules with tailored shapes. *Nature* **513**, 183–188 (2014).
45. Ganić, A. & Pfaltz, A. Iridium-catalyzed enantioselective hydrogenation of alkenylboronic esters. *Chem. Eur. J.* **18**, 6724–6728 (2012).
46. Xi, Y. & Hartwig, J. F. Diverse asymmetric hydrofunctionalization of aliphatic internal alkenes through catalytic regioselective hydroboration. *J. Am. Chem. Soc.* **138**, 6703–6706 (2016).
47. Zhang, L. et al. Catalytic conjunctive cross-coupling enabled by metal-induced metallate rearrangement. *Science* **351**, 70–74 (2016).
48. Schmidt, J., Choi, J., Liu, A. T., Slusarczyk, M. & Fu, G. C. A general, modular method for the catalytic asymmetric synthesis of alkylboronate esters. *Science* **354**, 1265–1269 (2016).
49. Stoltz, B. M. et al. Potassium *tert*-butoxide-catalyzed dehydrogenative C–H silylation of heteroaromatics: a combined experimental and computational mechanistic study. *J. Am. Chem. Soc.* **139**, 6867–6879 (2017).
50. Wynn, D. A., Roth, M. M. & Pollard, B. D. The solubility of alkali-metal fluorides in non-aqueous solvents with and without crown ethers, as determined by flame emission spectrometry. *Talanta* **31**, 1036–1040 (1984).
51. Chen, Z.-M., Hilton, M. J. & Sigman, M. S. Palladium-catalyzed enantioselective redox-relay Heck arylation of 1,1-disubstituted homoallylic alcohols. *J. Am. Chem. Soc.* **138**, 11461–11464 (2016).
52. Sawamura, M. & Ito, Y. Catalytic asymmetric synthesis by means of secondary interaction between chiral ligands and substrates. *Chem. Rev.* **92**, 857–871 (1992).
53. Corriu, R. J. P., Guerin, C., Henner, B. & Wang, Q. Pentacoordinate hydridosilicates: synthesis and some aspects of their reactivity. *Organometallics* **10**, 2297–2303 (1991).
54. Bandar, J. S., Pirnot, M. T. & Buchwald, S. L. Mechanistic studies lead to dramatically improved reaction conditions for the Cu-catalyzed asymmetric hydroamination of olefins. *J. Am. Chem. Soc.* **137**, 14812–14818 (2015).
55. Huo, H., Gorsline, B. J. & Fu, G. C. Catalyst-controlled doubly enantioconvergent coupling of racemic alkyl nucleophiles and electrophiles. *Science* **367**, 559–564 (2020).
56. Frampton, J. E. Pregabalin: a review of its use in adults with generalized anxiety disorder. *CNS Drugs* **28**, 835–854 (2014).
57. Mujahid, M. & Muthukrishnan, M. A new enantioselective synthesis of the anticonvulsant drug pregabalin (Lyrica) based on a hydrolytic kinetic resolution method. *Chirality* **25**, 965–969 (2013).
58. Zheng, B. & Srebnik, M. Preparation and selective cleavage reactions of boron-zirconium 1,1-bimetalloalkanes. *Tetrahedron Lett.* **34**, 4133–4136 (1993).
59. Gutierrez, O., Tellis, J. C., Primer, D. N., Molander, G. A. & Kozlowski, M. C. Nickel-catalyzed cross-coupling of photoredox-generated radicals: uncovering a general manifold for stereoconvergence in nickel-catalyzed cross-couplings. *J. Am. Chem. Soc.* **137**, 4896–4899 (2015).

Methods

General procedure for probing the scope of enantioselective C(sp^3)–C(sp^3) cross-coupling of non-activated alkyl electrophiles. To an oven-dried, 10 ml Teflon screw-capped test tube were added $NiCl_2$ (1.9 mg, 15 µmol, 0.15 equiv.) and **L6** (5.8 mg, 0.02 mmol, 0.20 equiv.). The vial was placed in a nitrogen-filled glovebox. A magnetic stir bar (6 × 15 mm), anhydrous DCE (0.30 ml) and DMF (0.20 ml) were added and the mixture was stirred for 40 min at room temperature. Then anhydrous KF (14.5 mg, 0.25 mmol, 2.50 equiv.) was added and the stirring was continued for an additional 2–3 min, at which point alkenyl boronic acid pinacol ester **1** (0.15 mmol, 1.00 equiv.) was added and the mixture stirred for an additional 1 min. Then alkyl iodide **2** (0.10 mmol, 1.50 equiv.) was added to the resulting mixture [for cross-coupling with secondary alkyl iodides: alkenyl boronic acid pinacol ester **1** (0.10 mmol, 1.00 equiv.) and secondary alkyl iodide (0.15 mmol, 1.50 equiv.) were used]. Stirring was further continued for 5 min, then DEMS (43.0 µl, 0.25 mmol, 2.50 equiv.) was added dropwise to it. The test tube was then sealed with airtight electrical tape and removed from the glove box and stirred at RT for 40 h maintaining 460 r.p.m. The crude reaction mixture was directly subjected to flash column chromatography using a mixture of hexane and EtOAc to obtain **3a**–**6i**.

Data availability

Crystallographic data for **3e**′ and **4g**′ have been deposited at the Cambridge Crystallographic Data Centre, under deposition numbers CCDC 2011678 (**3e**′) and CCDC 1971802 (**4g**′). Copies of the data can be obtained free of charge via www.ccdc.cam.ac.uk. All other data supporting the findings of this study, including experimental procedures and compound characterization, NMR, HPLC and X-ray analyses are available within the Article and its Supplementary Information.

Acknowledgements

This work is supported by the Swiss National Science Foundation. We thank F. Fadaei Tirani for the determination of the X-ray crystal structures of compounds **3e**′ and **4g**′.

Author contributions

S.B. and X.H. conceived the project. S.B. designed and optimized the synthetic method. S.B. and R.M. studied the scope, application and mechanism. All authors analysed the data and co-wrote the manuscript. X.H. directed the research.

Competing interests

The authors declare no competing interests.

Additional information

Supplementary information is available for this paper at https://doi.org/10.1038/s41557-020-00576-z.

Correspondence and requests for materials should be addressed to X.H.

Reprints and permissions information is available at www.nature.com/reprints.